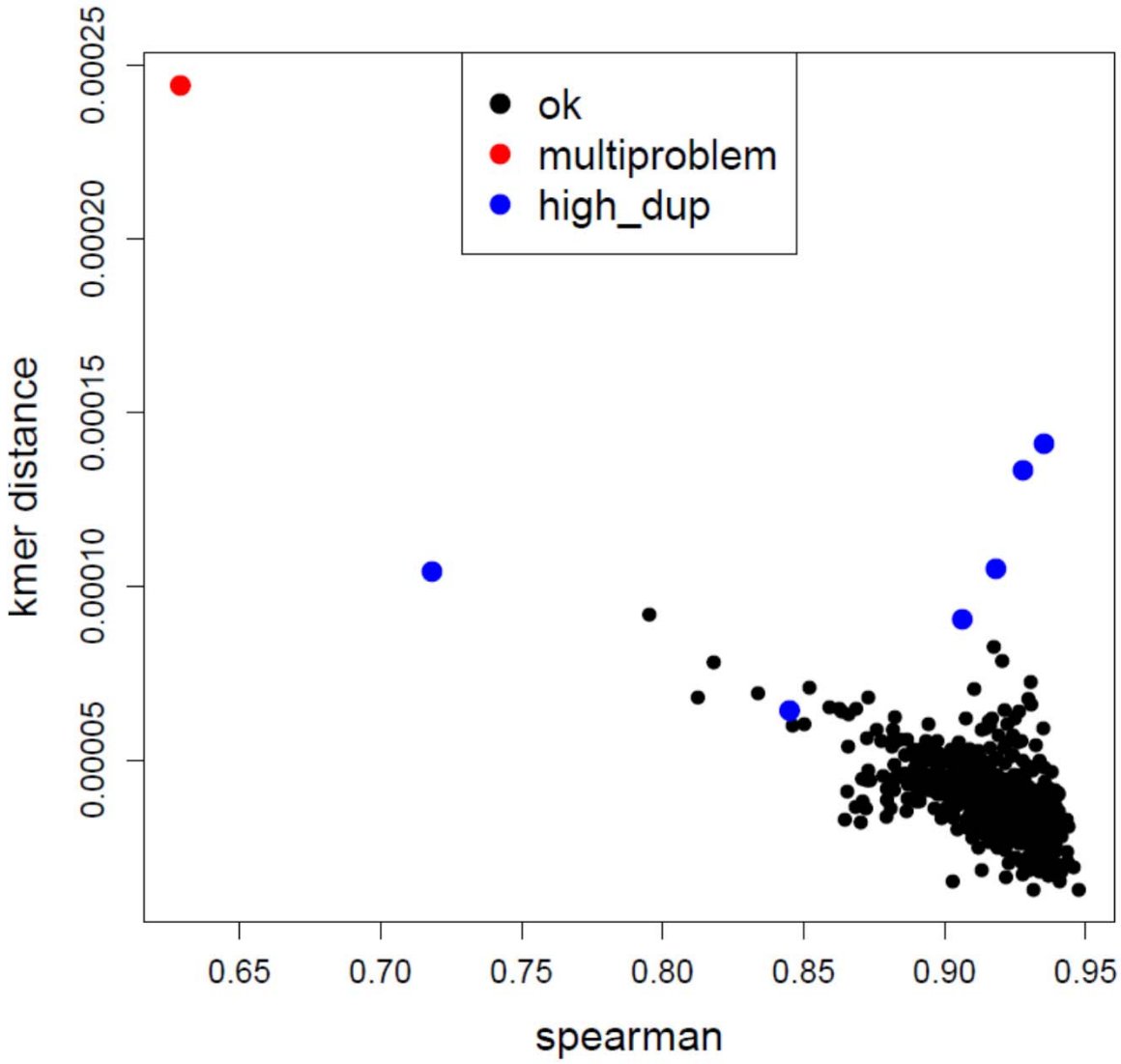

Suppl. Figure 1: Median of all pairwise Spearman correlations per sample based on exon quantifications (x-axis) plotted against median of k-mer distance (k=9) based on raw sequence reads. In red the sample NA18861.4 which failed all QC tests; in blue samples with high read duplication rates and/or high rRNA content.

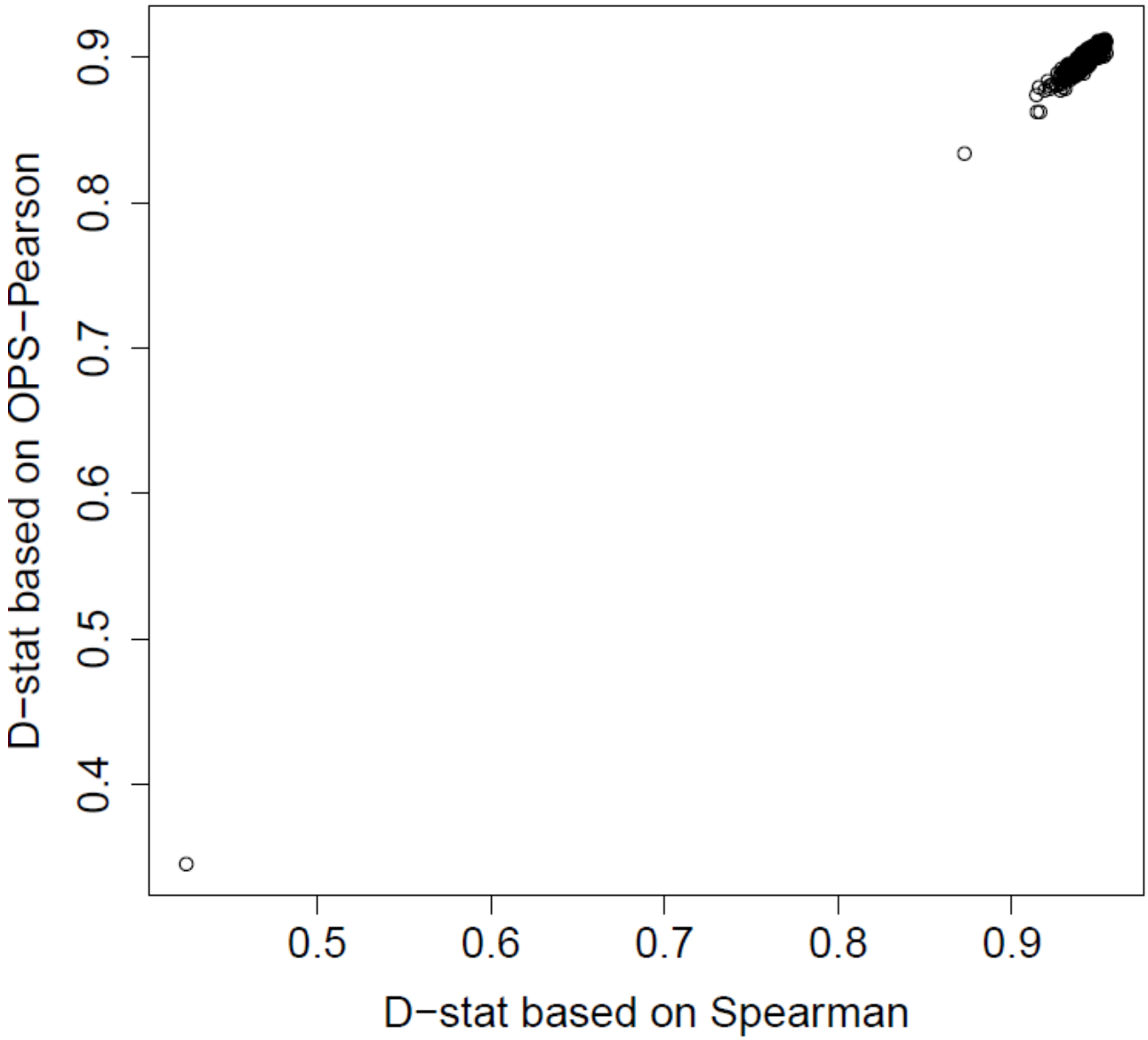

Suppl. Figure 2: D-statistics (median of all pairwise correlations per sample) for exon quantifications calculated from Pearson correlations after OPS transformation (i.e. raising all transcript quantifications to the power of 0.11) (y-axis) plotted against D-statistics calculated from Spearman correlations (x-axis). We found that Pearson product-moment coefficients derived from OPS-transformed data are agreeing well with Spearman's rank correlation computed on raw data, but with the additional advantage that the actual expression levels - and not solely their ranking - are taken into account.

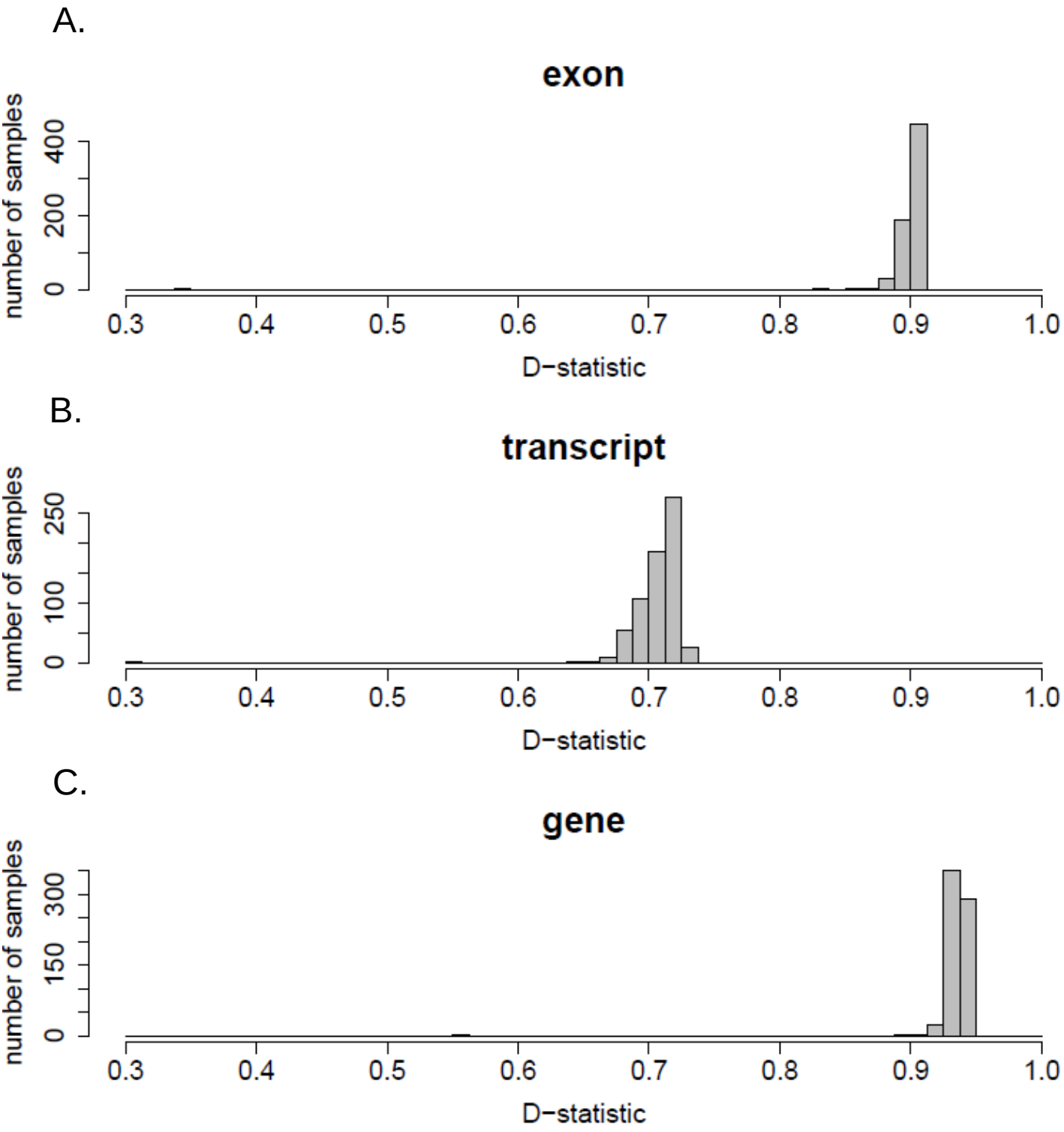

Suppl. Figure 3: Histogram of D-statistics (median of all pairwise correlations per sample) for exon (A), transcript (B) and gene quantifications (C), as calculated from Pearson correlations after OPS transformation.

A.

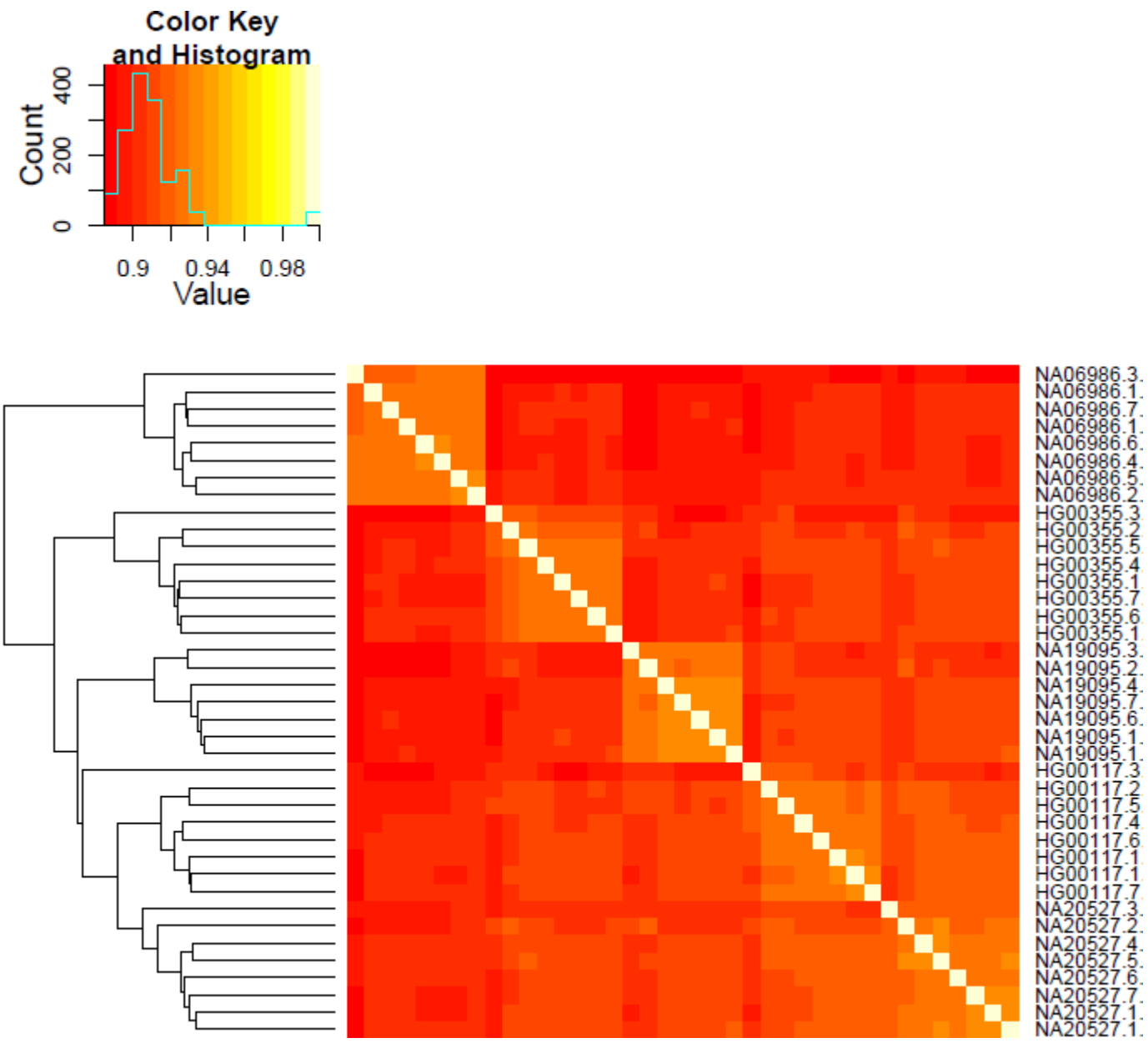

Suppl. Figure 4A: Heatmap and clustering of Pearson correlations (after OPS transformation) for exon quantifications. Color scale is indicated. Samples are indicated with their HapMap identifier followed by their sequence laboratory identifier. Sequence runs in different laboratories cluster by sample rather than by laboratory.

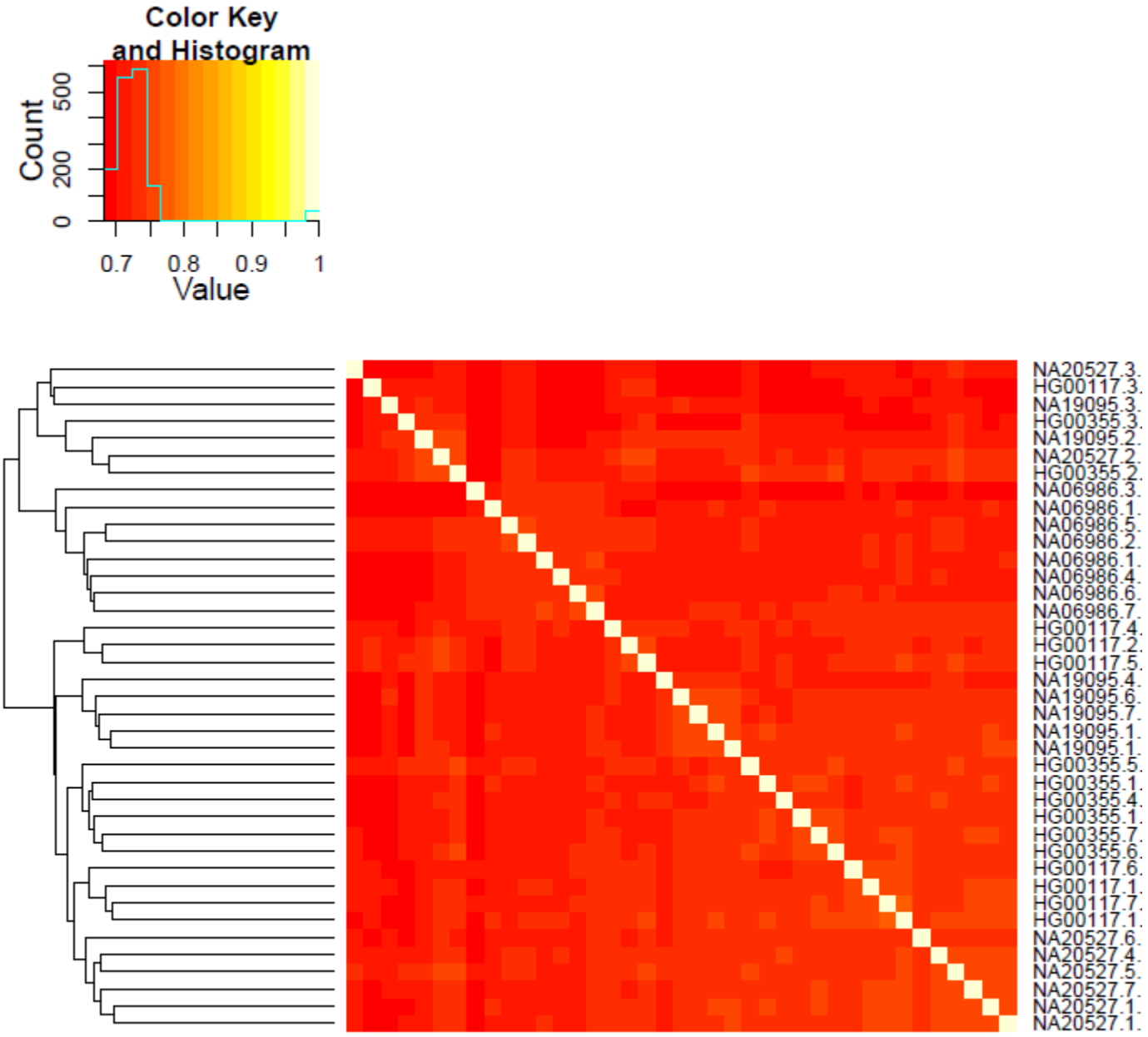

Suppl. Figure 4B: Heatmap and clustering of Pearson correlations (after OPS transformation) for transcript quantifications. Color scale is indicated. Samples are indicated with their HapMap identifier followed by their sequence laboratory identifier. Sequence runs in different laboratories generally cluster by sample rather than by laboratory. The intra-sample correlations are higher for exon than for transcript quantifications.

A.

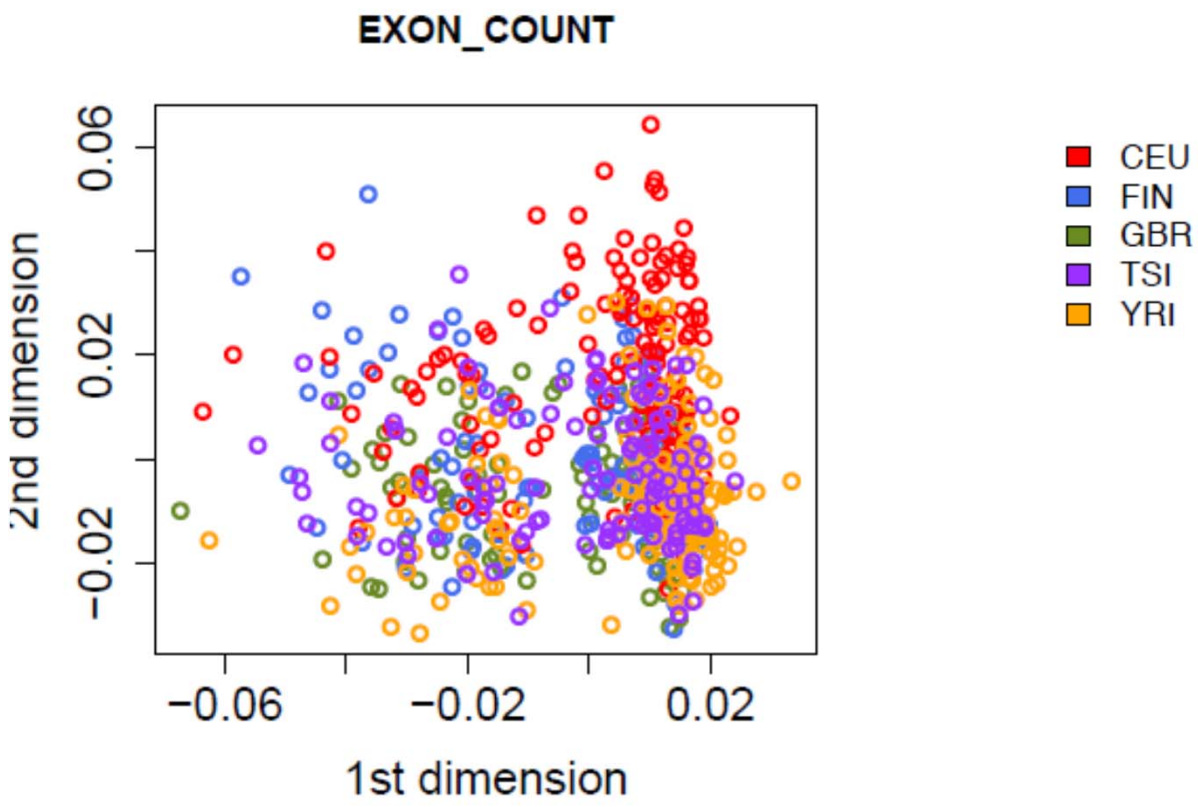

B.

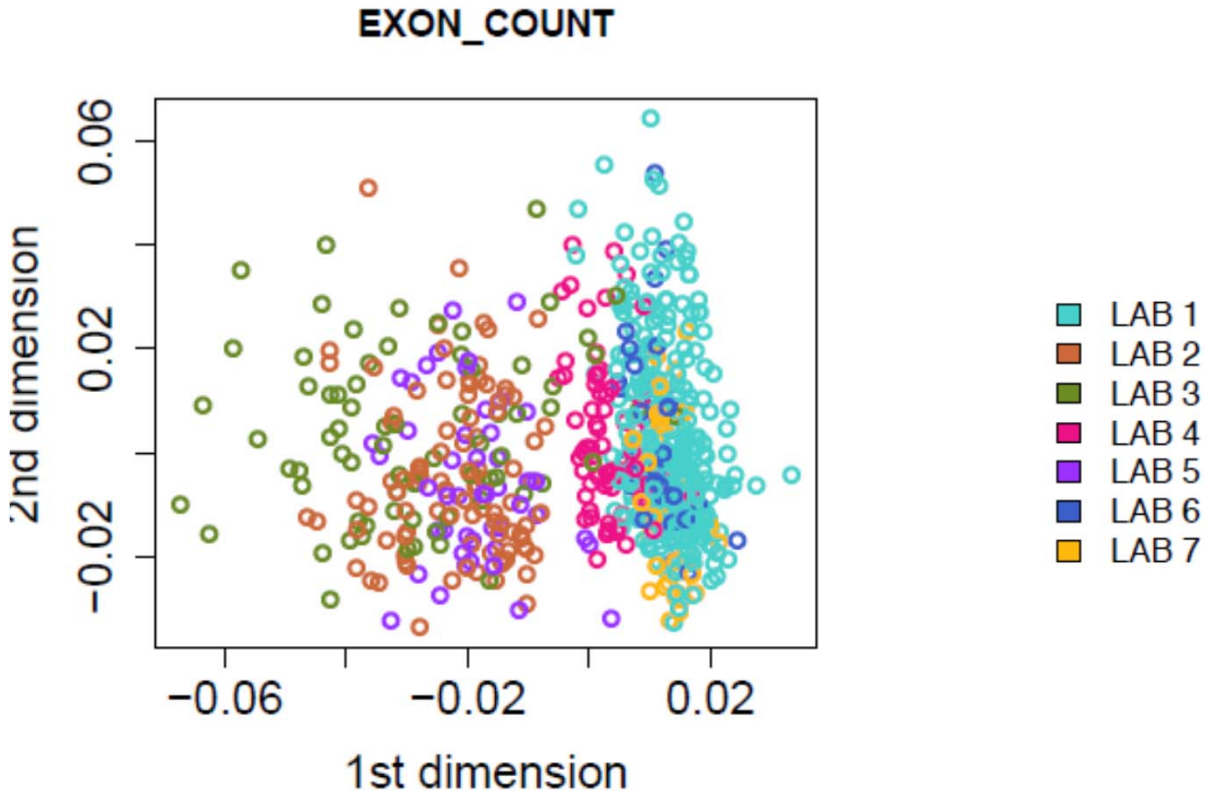

Suppl. Figure 5: Multidimensional scaling of pairwise sample correlations (Pearson correlations after OPS) based on exon quantifications colored by population (A) or laboratory (B).

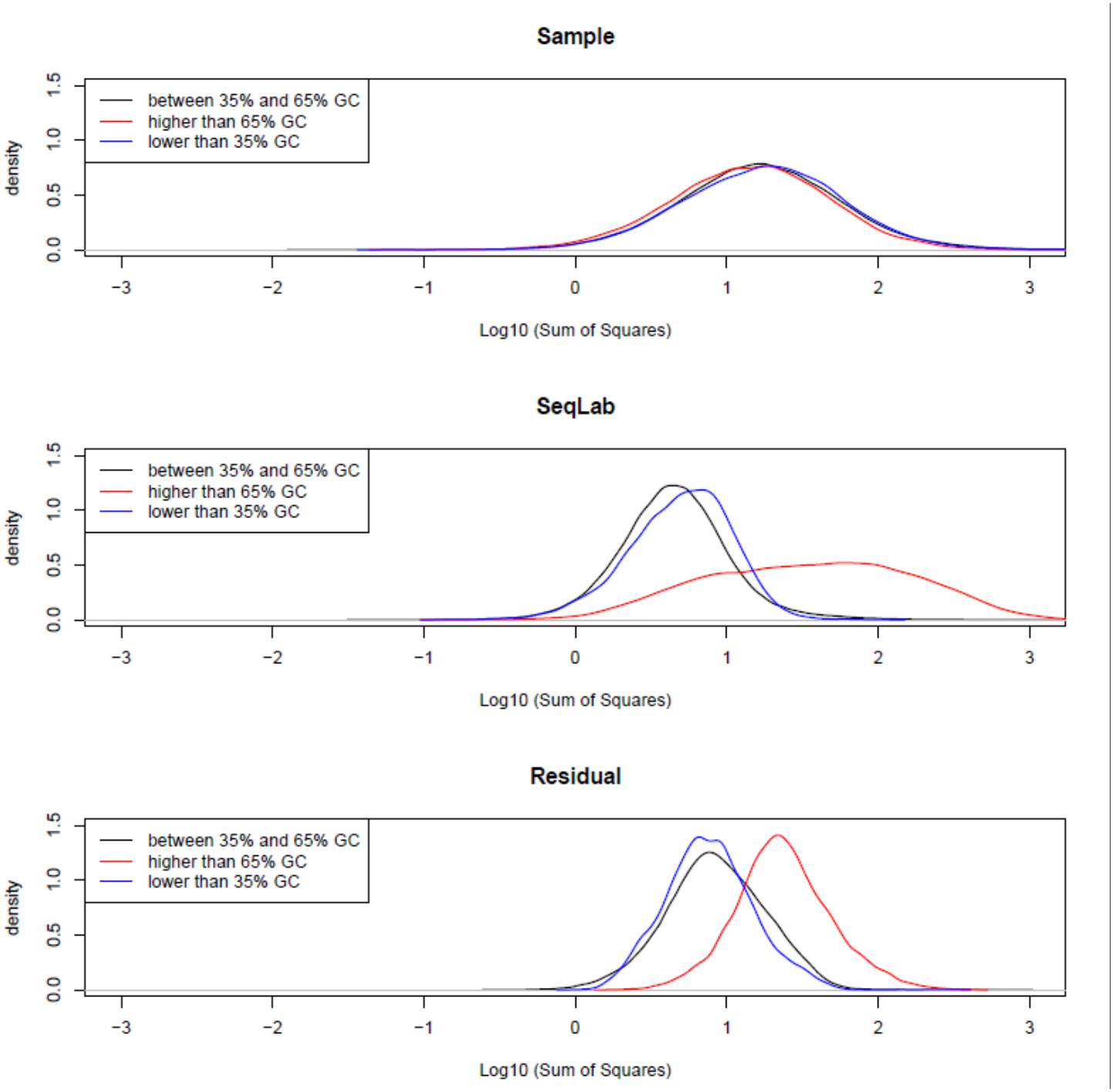

Suppl. Figure 6A: Effect of exonic GC percentage on sample and laboratory variation. We applied a linear model on the variance stabilized exon quantifications of the five samples replicated in each laboratory (see also our legend to Figure 3 of the main paper) and performed an analysis of variance for the factors Sample and sequencing laboratories (SeqLab). We distinguished exons with low GC (<35%, blue line), high GC (>65%, red line) and medium GC (between 35% and 65%). The density curves reflect the distribution of the sum of squares for Sample (top panel), Seqlab (middle panel) and the residual sum or squares (lower panel). Exons with >65% GC display clearly increased variation resulting from the laboratory as well as increased residual variation.

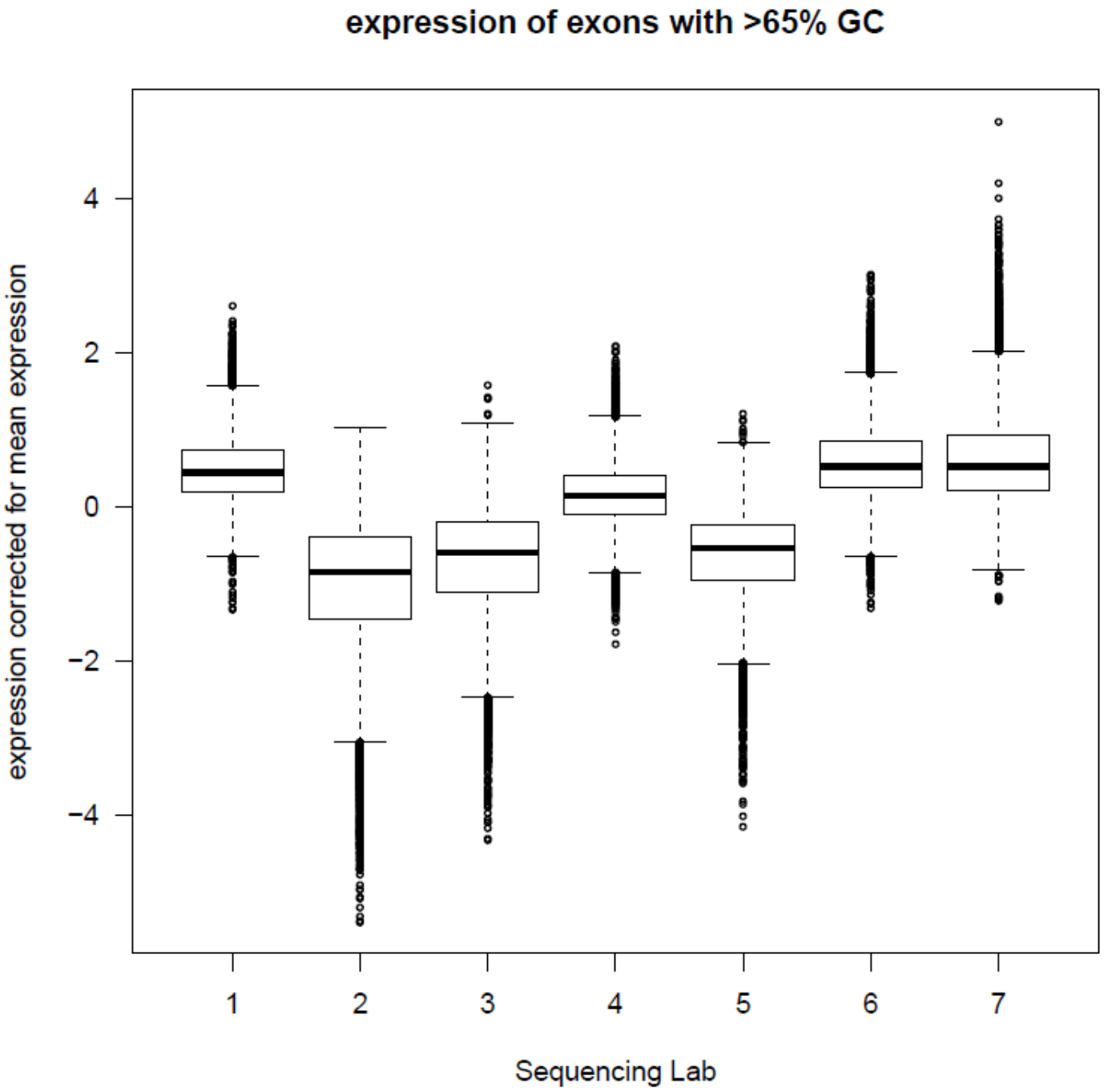

Suppl. Figure 6B: Expression of exons with >65% GC in the different sequencing laboratories corrected for the mean expression of that exon across all laboratories. Analysis was performed on the variance stabilized exon quantifications of the five samples replicated in each laboratory. Laboratories with broader GC coverage (main Figure 3E), also have higher expression of this subset exons. The use of PCR machines with lower ramp speeds contributed to better representation of GC-rich exons: Lab 1: Biometra (ramp speed 4°C/s); Lab 2: MasterCycler pro S from Eppendorf (Fast mode; 8°C/s); Lab 5: PeqSTAR 96 Universal (5°C/s); Lab 6: Applied Biosystems Verity (3-4°C/s); Lab 7: BioRad Tetrad2 (3°C/s).

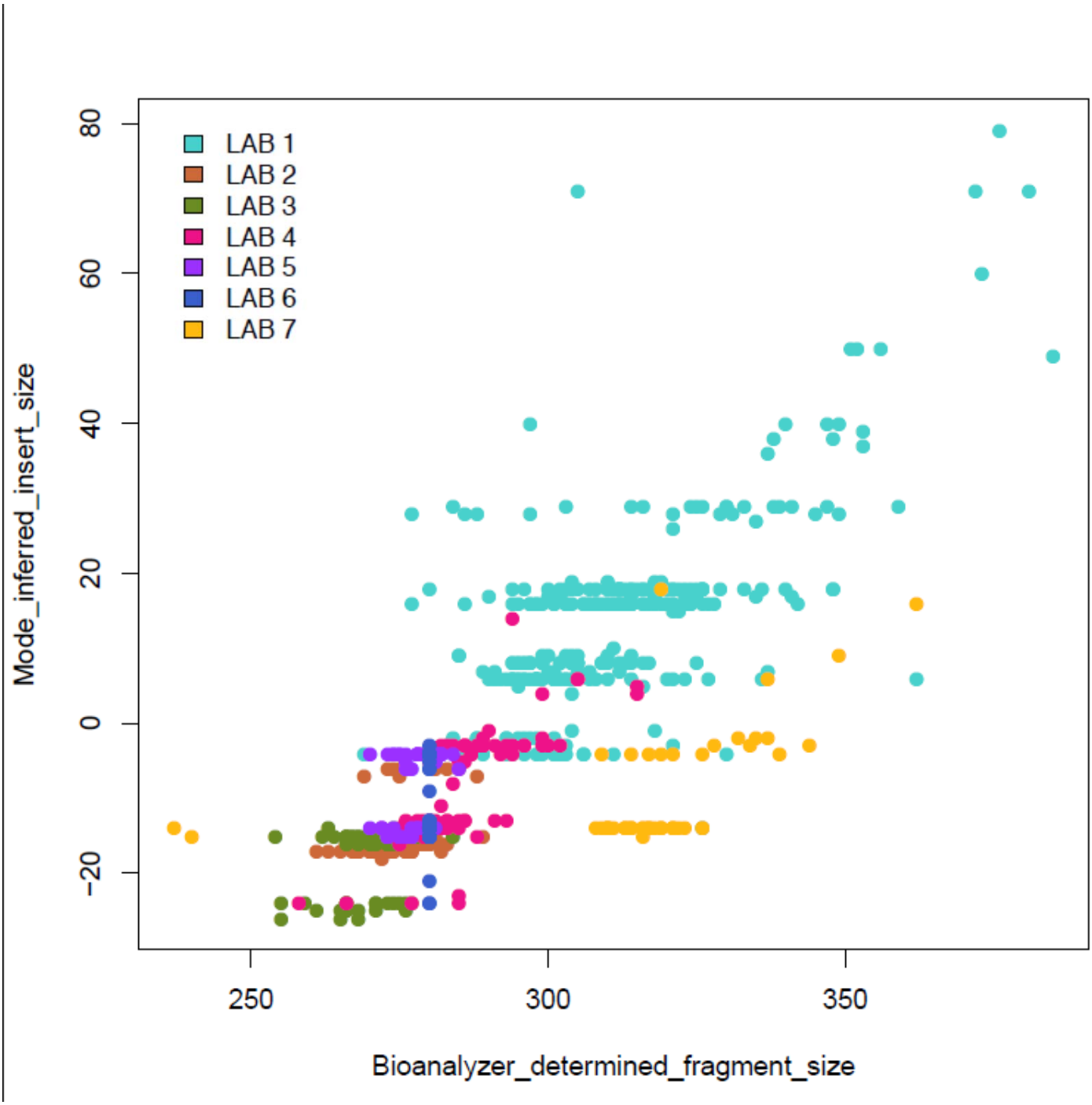

Suppl. Figure 7: Correlation between the Bioanalyzer determined fragment size (x-axis, including 120 nucleotides of adapter sequence) and the mode of the inferred insert size after alignment (y-axis, 0 corresponds with an insert size of 2x75 = 150 nucleotides). Dots are colored according to laboratory using our conventional color scheme. Lab number 7 deviates from the other laboratories, likely due to the use of high-sensitivity chips, while other laboratories used the DNA 1000 chip.

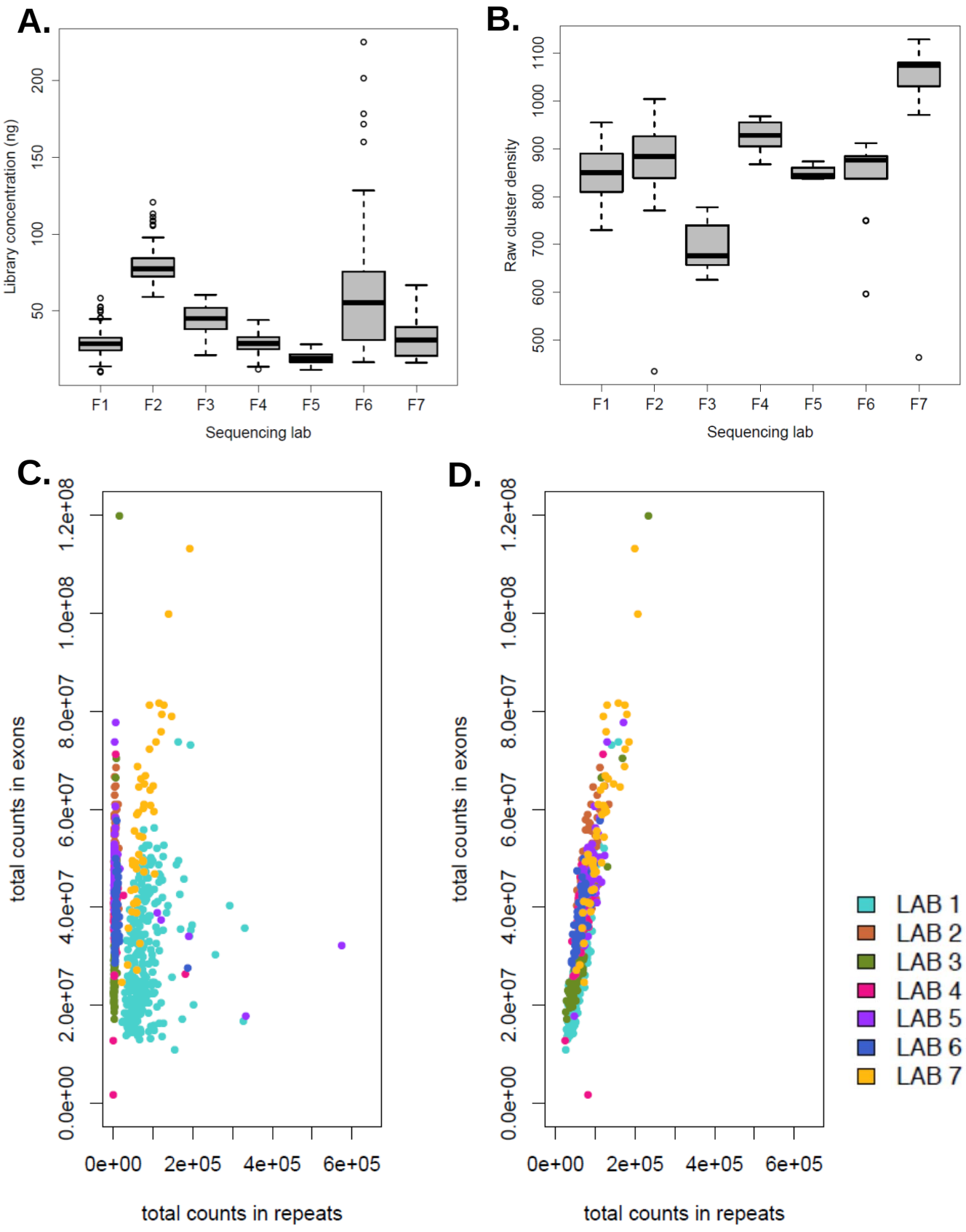

Suppl. Figure 8: Additional sample preparation differences between laboratories. A. Boxplot of library concentrations across different laboratories; B. Boxplot of raw cluster densities across different laboratories; C. Sum of the number of reads in repetitive regions outside genes (based on RepeatMasker, see Lappalainen et al., submitted) (x-axis) plotted against the sum of the counts in exons (y-axis) for all samples, colored according to the laboratory. D. same as C, but now counts in rRNAs are not included in the repeat counts.

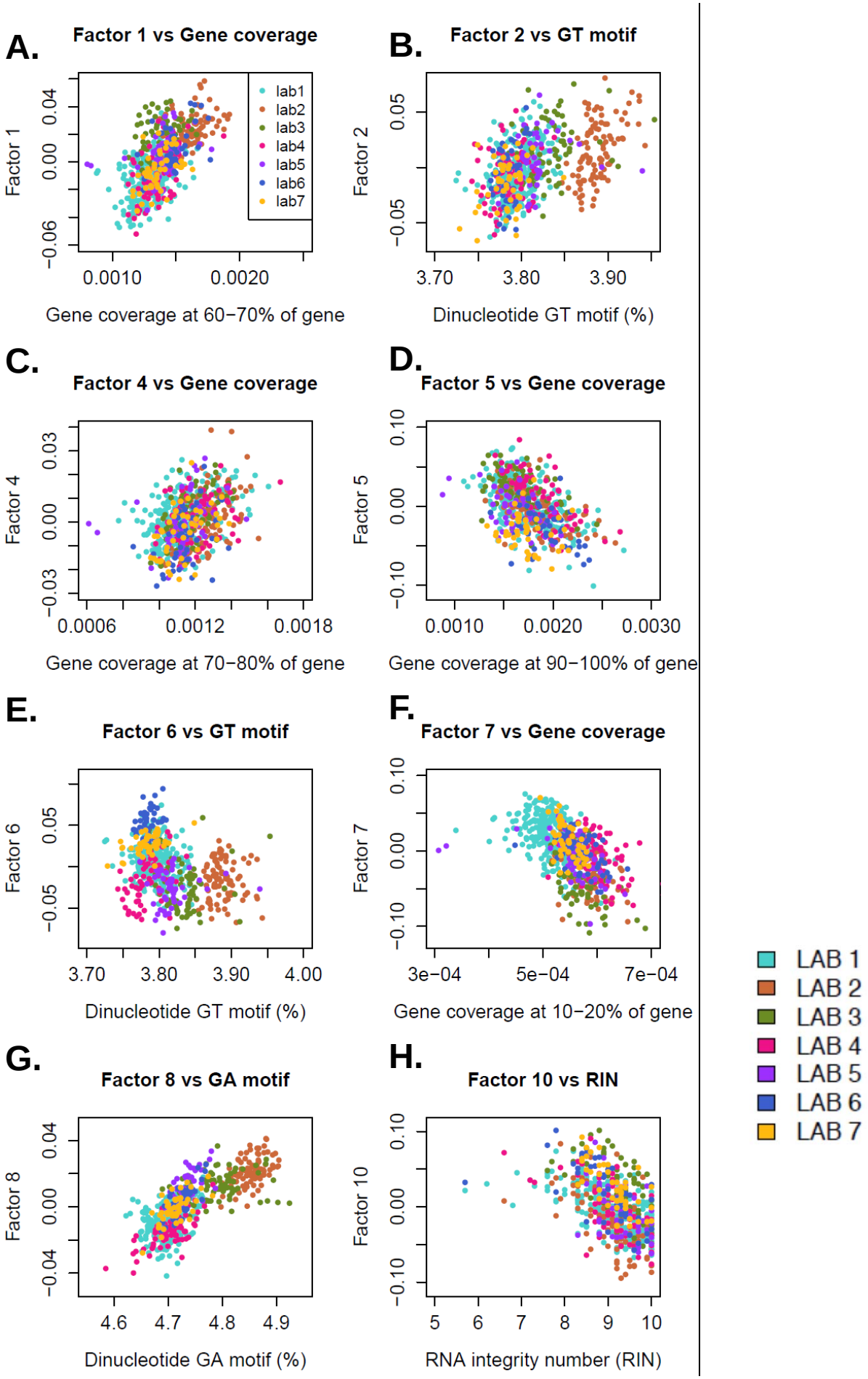

Suppl. Figure 9A: Correlation of sample characteristics most strongly associated with PEER components 1 (A), 2 (B), 4 (C), 5 (D), 6 (E), 7 (F), 8 (G), and 10 (H), colored by laboratory.

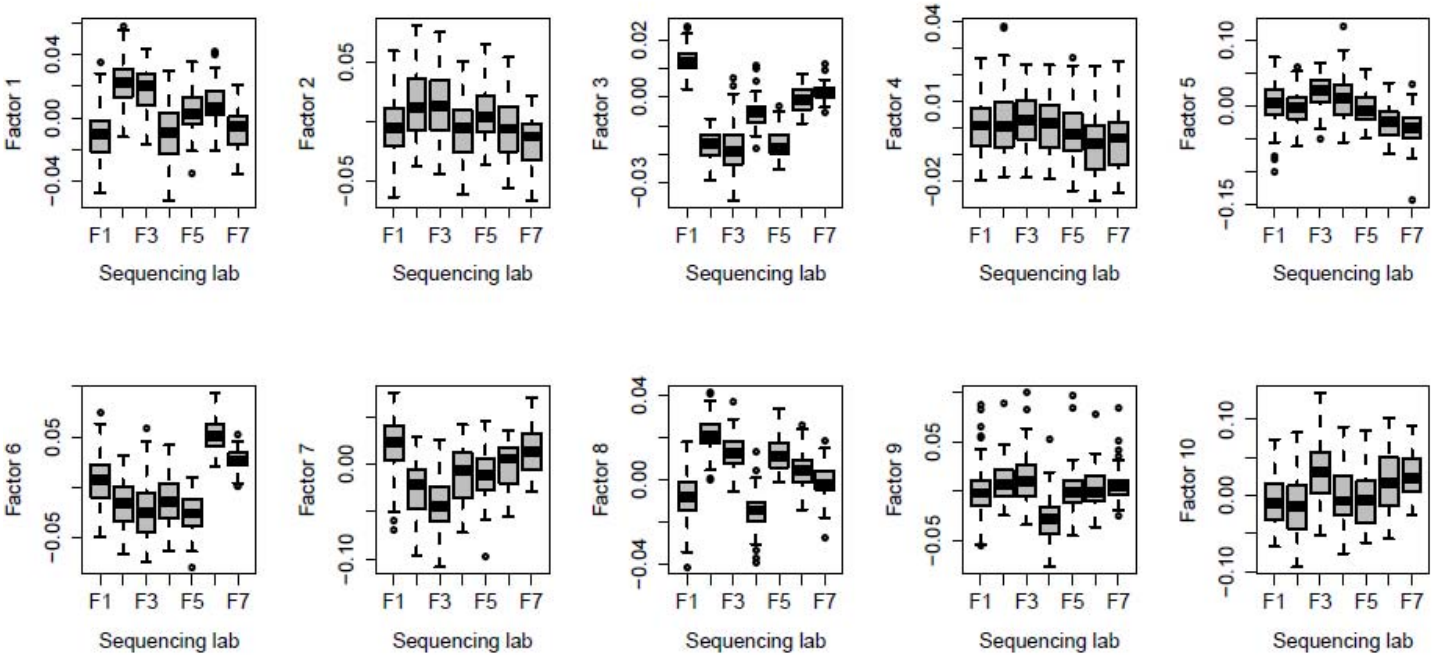

Suppl. Figure 9B: Boxplots of the distribution of values of the 10 PEER components over the laboratories, showing the large contribution of interlaboratory variation to PEER factors 1, 3, 6, 7, and 8.

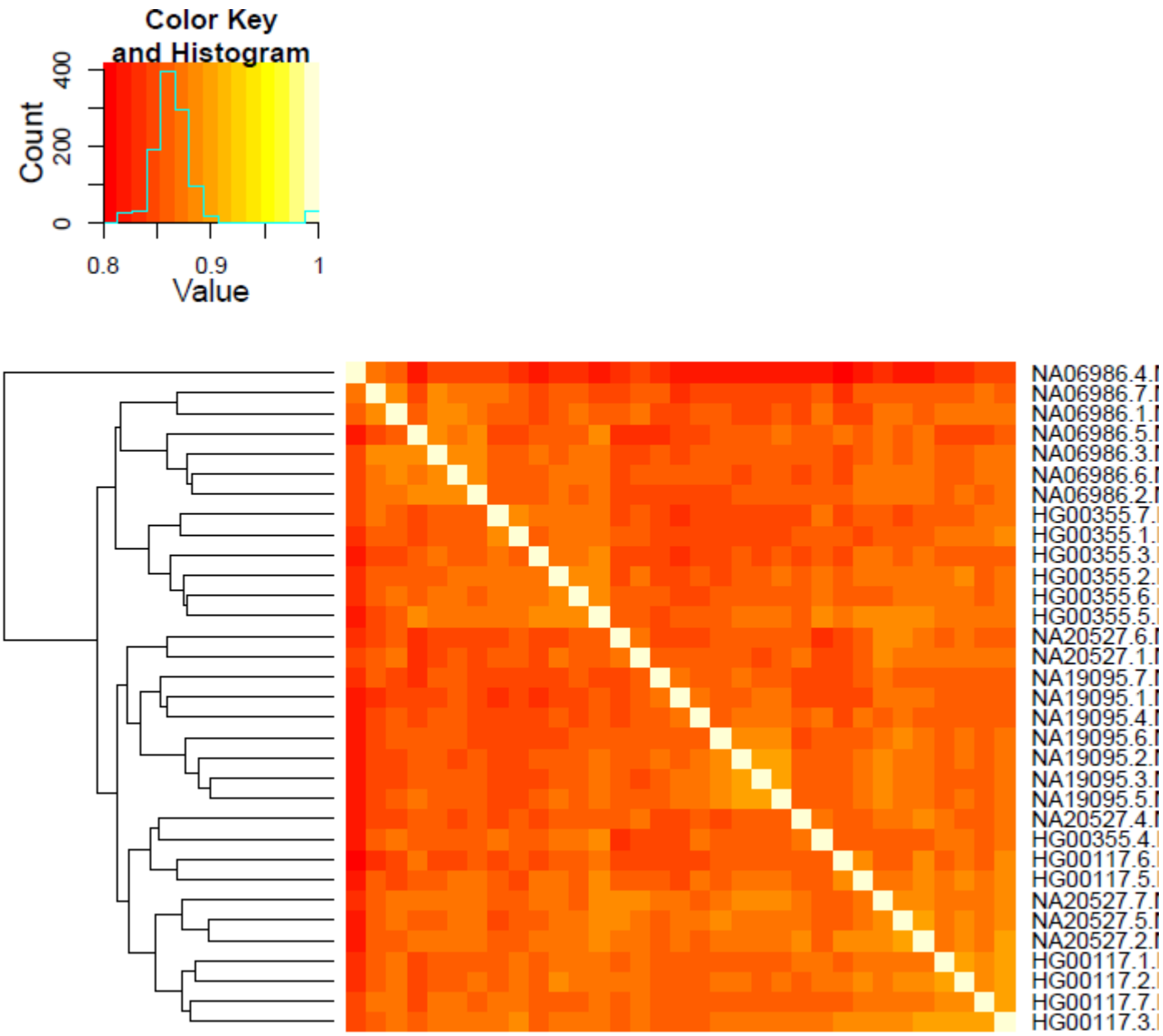

Suppl. Figure 10: Heatmap and clustering of Pearson correlations (after OPS transformation) for miRNA quantifications. Color scale is indicated. Samples are indicated with their HapMap identifier followed by their sequence laboratory identifier.

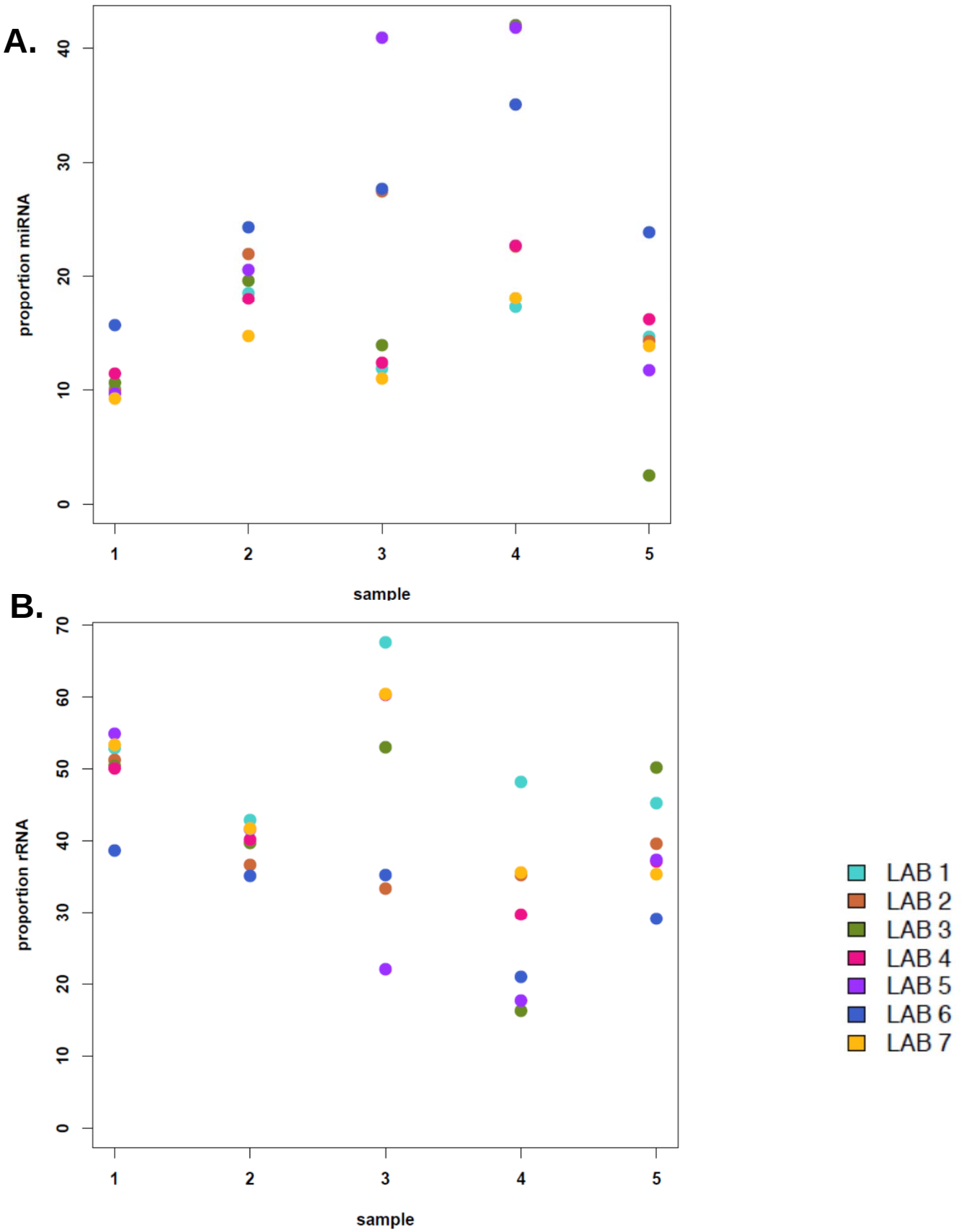

Suppl. Figure 11: Proportion of miRNA (A) and rRNA (B) reads in the five samples replicated in all seven sequencing laboratories (indicated with different colors). Analysis of variance demonstrated a larger contribution of the sample than the laboratory (41% vs 22 % of miRNA content explained by sample and lab, respectively, and 38% vs 26% of rRNA content explained by sample and lab, respectively). Only the sample effect is significant. This indicates that differences in the relative proportion of small RNAs have been introduced before the preparation of the samples for sequencing.

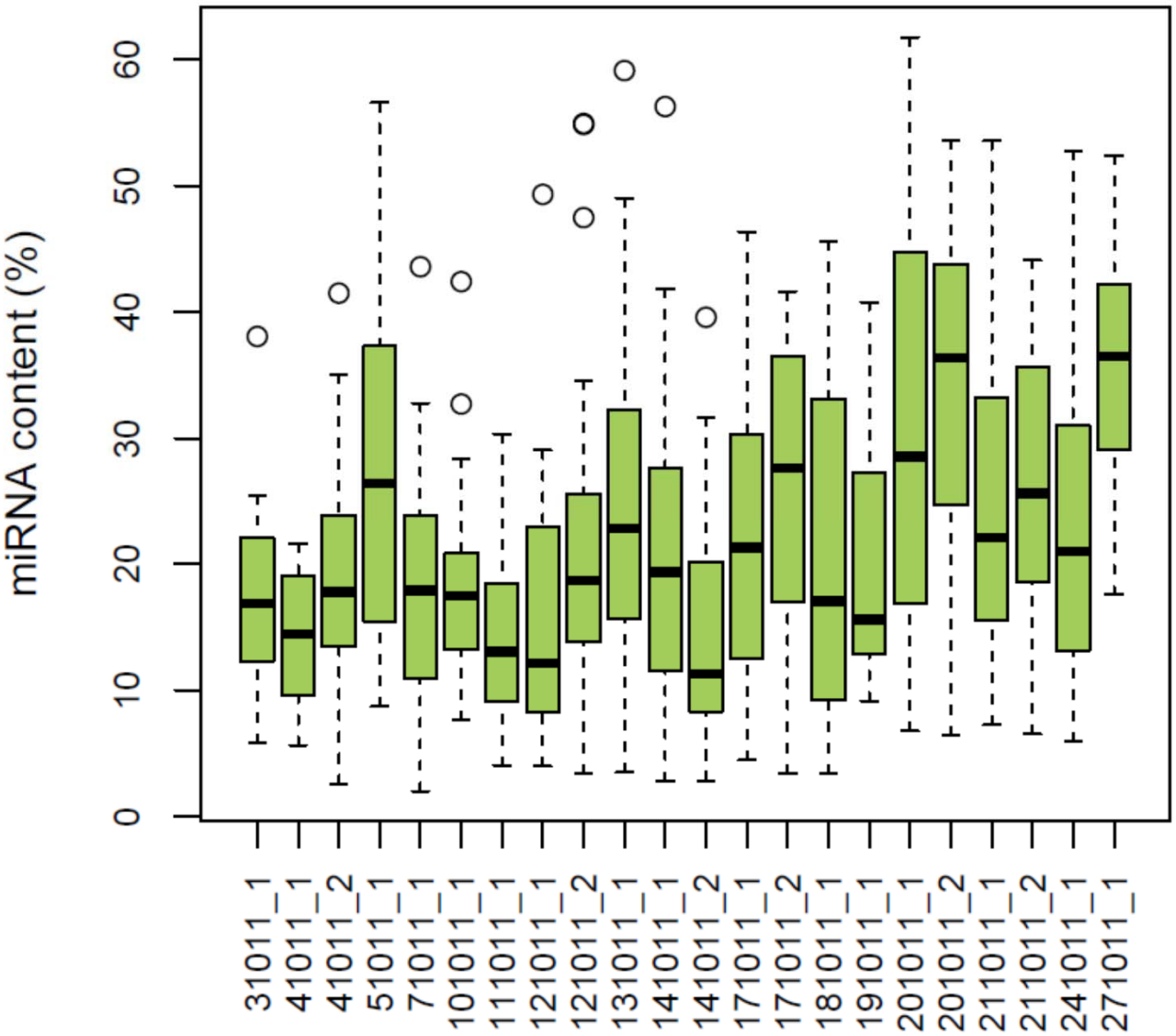

Suppl. Figure 12: Proportion of miRNA of the total number of mapped small RNA reads in different RNA extraction batches.

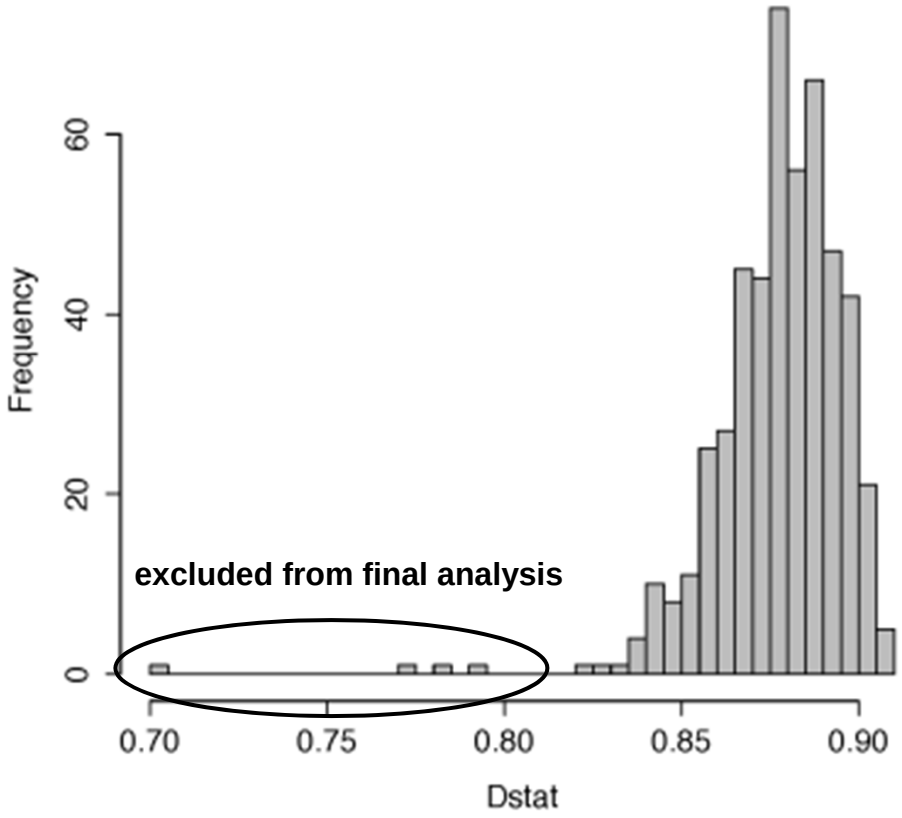

Suppl. Figure 13: Histogram of D-statistics (median of pairwise Pearson correlation after OPS transformation) for miRNA quantifications

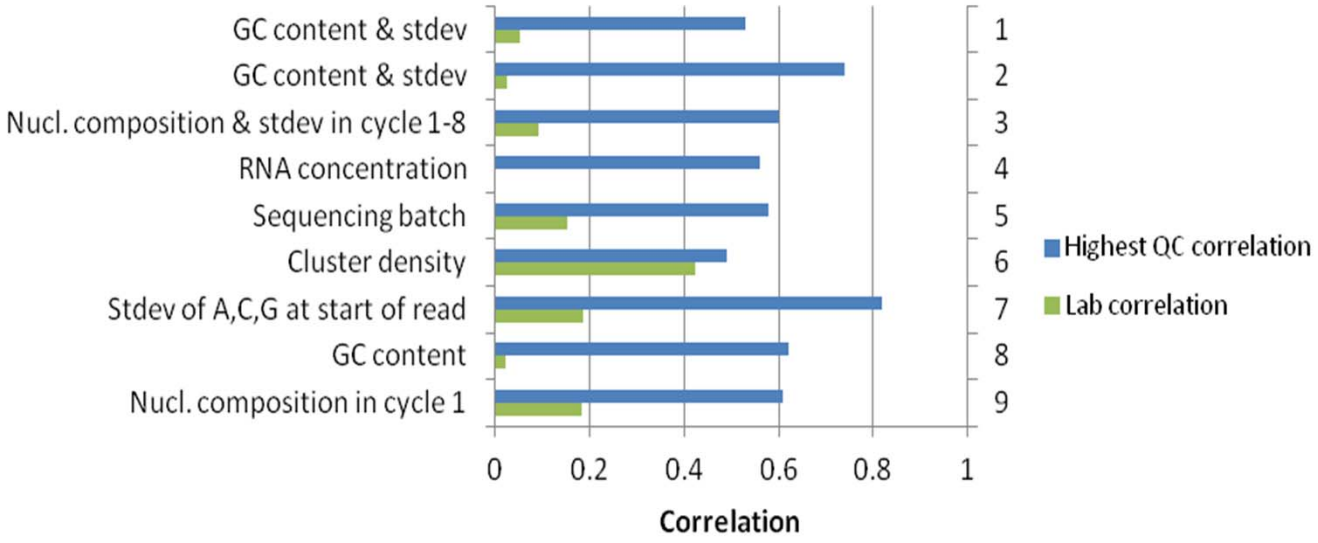

Suppl. Figure 14: Most important sources of miRNA sample variation for each PEER factor, strength of these correlations (blue bars) and the correlation of the laboratory effect to each PEER factor (green bars). For numerical factors Spearman correlations are shown. For categorical variables the categories are first transformed into factors that are used together with each PEER factor in a linear regression. From the linear regression the R2 value is extracted and used to measure the correlation.